A&A 397, 883–890 (2003)
DOI: 10.1051/0004-6361:20021574

Astronomy & Astrophysics

XMM–Newton observations of the Seyfert 1 galaxy NGC 3227

P. Gondoin, A. Orr, D. Lumb, and H. Siddiqui

Research and Scientific Support Department, European Space Agency – Postbus 299, 2200 AG Noordwijk, The Netherlands

Received 1 May 2002 / Accepted 30 October 2002

Abstract. We report on an *XMM–Newton* observation of the Seyfert 1 galaxy NGC 3227 performed in November 2000. The observed X-ray spectrum above 4 keV is well fitted by a hard power law continuum ($\Gamma \approx 1.5$) and an absorption edge at 7.6 keV. An Fe K emission line with an equivalent width of 213 eV is detected at 6.4 keV. The line is narrow suggesting contribution from material in low ionization states (<Fe XVII) relatively far from a central black hole. The continuum is strongly absorbed at soft energies by a column of neutral gas ($\approx 6.5 \times 10^{22}$ cm^{-2}) larger than previously measured and covering a significant fraction (≈90%) of the central source. The soft X-ray continuum is also attenuated due to the presence of ionized material ($\xi \approx 50-90$ erg s^{-1} cm) suggesting the presence of a substantial amount of gas ($N_{\rm H} \approx 2-9 \times 10^{21}$ cm^{-2}) in the vicinity (<0.4 pc) of the nucleus. We find that NGC 3227 exhibits significant spectral variability above 2 keV on time scales of a few ksec during the *XMM–Newton* observations. This short term variability is likely related to variation in the continuum emission. Comparisons with previous observations indicate that variability on timescale of a month also involves a change in the column densities of neutral absorbing material along the line of sight to the nucleus.

Key words. galaxies: individual: NGC 3227 – galaxies: nuclei – galaxies: Seyfert

1. Introduction

NGC 3227 is a nearby Sb galaxy at a redshift $z = 0.00386$ (Crenshaw et al. 2001) with an active nucleus usually classified as a Seyfert 1.5 (Oosterbrock & Martel 1993). It shows signs of interaction with its dwarf elliptical companion NGC 3226. NGC 3227 has been extensively studied in most regions of the electromagnetic spectrum. The optical emission lines and continuum from the active nucleus are known to be reddened (Cohen 1983; Winge et al. 1995). *IUE* spectra show that the UV continuum is also heavily reddened, as evidenced by the steep drop in continuum flux from near to far UV (Courvoisier & Paltani 1983). Observations of NGC 3227 with *HEAO1* indicated a strong variability in the X-ray domain. Tennant & Mushotzky (1983) found a 40% flux increase within 5 hours. Variability was also present in the *EXOSAT* data (Turner & Pounds 1989) and in an *ASCA* observation (Ptak et al. 1994). Differential variability between the *EXOSAT* LE (0.05–2 keV) and ME (2–10 keV) instruments was interpreted in terms of either partial covering with a strongly varying cold column or a variable soft-excess (Turner & Pounds 1989).

An iron-K emission line near 6.5 keV was detected in the *GINGA* spectrum of NGC 3227 (Pounds et al. 1989). George et al. (1990) analysed this observation within the frame of a model of reflection from a cold accretion disk. The underlying continuum emission was then best described by a power law with a photon index $\Gamma = 1.86$. Evidence for the presence of a warm absorber in NGC 3227 was indicated by Netzer et al. (1993) and Ptak et al. (1994) in an *ASCA* observation. In addition to the warm absorber, Komossa & Fink (1997) and George et al. (1998) found that a column density of $\leq 3 \times 10^{20}$ cm^{-2} of neutral material in addition to the Galactic column ($\approx 2.1 \times 10^{20}$ cm^{-2}; cf. Murphy et al. 1996), is required to model the X-ray spectrum below 500 eV. This intrinsic column of gas in the line of sight to NGC 3227 is not sufficient to produce the observed reddening, assuming a Galactic dust to gas ratio ($N_{\rm H1} = 5.2 \times 10^{21}\ E_{B-V}$ cm^{-2}; Shull & van Steenberg 1985). A higher column density ($\approx 6 \times 10^{20}$ cm^{-2}) has been suggested based on 21 cm VLA observations (Mundell et al. 1997). However, the angular resolution of the VLA data is 12″ (≈850 pc) and Mundell et al. (1997) did not detect H I absorption directly against the radio continuum source in the inner nucleus. Komossa & Fink (1997) concluded that a dusty warm absorber is present in NGC 3227 where the dust exists within the highly ionized X-ray absorber. In a paper on the reddening in X-ray absorbed Seyfert 1 galaxies, Kraemer et al. (2000) propose a component of dusty gas with an ionization state such that hydrogen is nearly completely ionized but that the O VII and O VIII columns are negligible. Using a combined *ROSAT*/*ASCA* dataset, Kraemer et al. (2000) argue that such a component lying outside the Narrow Line Region (NLR) could explain both the reddening of the optical continuum and narrow lines and the attenuation of the X-ray spectrum below 500 eV.

In the present paper, we report the analysis results of *XMM–Newton* observations of NGC 3227 performed in November 2000. Section 2 details the observations and data reduction procedures. Section 3 presents the integrated flux measurements and their temporal behaviour during the

Send offprint requests to: P. Gondoin,
e-mail: pgondoin@rssd.esa.int

observations. Section 4 describes the spectral analysis which was performed in two steps including first a characterization of the continuum emission above 4 keV and of the Fe K spectral features around 6.4 keV and then an analysis of the entire 0.3–10 keV energy range. The results are discussed in Sect. 5.

2. Observations and data reduction

NGC 3227 was observed by the *XMM–Newton* space observatory (Jansen et al. 2001) between 2000 November 28 18:10:23 (UT) and 2000 November 29 05:25:18 (UT) for usable exposure times of 35.3 ksec (EPIC p−n camera) and 37.4 ksec (EPIC MOS 1 and MOS 2 cameras). *XMM–Newton* uses three grazing incidence telescopes which provide an effective area >4000 cm^2 at 2 keV and 1600 cm^2 at 8 keV (Gondoin et al. 2000). Three EPIC CCD cameras (Strüder et al. 2001; Turner et al. 2001) at the prime focus of the telescopes provide imaging in a 30′ field of view and broadband spectroscopy with a resolving power of between 5 and 60 in the energy range 0.3 to 10 keV. Two identical RGS reflection grating spectrometers behind two of the X-ray telescopes allow high resolution ($E/\Delta E$ = 100 to 500) measurements in the soft X-ray range (6 to 38 Å or 0.3 to 2.1 keV) with a maximum effective area of about 140 cm^2 at 15 Å (den Herder et al. 2001).

The observations of NGC 3227 were conducted with the EPIC cameras operating in full frame mode. RGS spectra were recorded simultaneously with a low signal to noise ratio due to the relative faintness of the source. "Medium" thickness aluminum filters were used in front of all CCD cameras to reject visible light. The raw event data sets were processed with the "emproc", "epproc" and "rgsproc" pipeline tasks of the *XMM–Newton* Science Analysis System (SAS version 5.2.0) in order to generate calibrated event lists. The source spectra in the EPIC cameras were built from photons detected within a circle of 37″ radius from the target boresight. The background was estimated on the same CCD chips within windows of similar size which were offset by about 3′ from the source centroid position. Background rates were low during the whole observation. The Pulse-Invariant (PI) spectra were rebinned such that each resultant channel had at least 50 counts per bin in the p-n spectra and 25 counts per bin in the MOS spectra. χ^2 minimization was used for the spectral fitting. All fits were performed using the XSPEC package (v11). We used EPIC response matrices provided by the PI institutes.

3. Integrated flux and temporal behaviour

The spectral analysis of the NGC 3227 data (see Sect. 4) yields flux measurements in the low (0.3−2 keV) and high (2−10 keV) energy bands of $F_{\rm LE} = (4.234 \pm 0.001) \times 10^{-13}$ erg $cm^{-2}\,s^{-1}$ and $F_{\rm HE} = (7.554 \pm 0.001) \times 10^{-12}$ erg $cm^{-2}\,s^{-1}$, respectively. After correction of the galactic absorption by hydrogen column density ($N_{\rm H} = 2.1 \times 10^{20}$ cm^{-2}; cf. Murphy et al. 1996), these correspond to luminosities of $L_{\rm LE} = 1.35 \times 10^{40}$ erg s^{-1} and $L_{\rm HE} = 21.6 \times 10^{40}$ ergs s^{-1} for $z = 0.00386$ and $H_0 = 75$ km s^{-1} Mpc^{-1}.

NGC 3227 is known as a variable low luminosity Seyfert 1 galaxy. *ASCA* observations performed during 1993 and 1995 provided 2–10 keV flux measurements in the range 2.42–2.64 × 10^{-11} erg $cm^{-2}\,s^{-1}$ (George et al. 1998). *Ginga* observations performed in 1988 indicated $F_{\rm HE} \approx 4.0 \times 10^{-11}$ erg $cm^{-2}\,s^{-1}$ (Pounds et al. 1989), close to the level of the *EXOSAT* spectral survey. The NGC 3227 flux in the 2–10 keV band during the *XMM–Newton* observations is in the lower end of the range of luminosities previously reported.

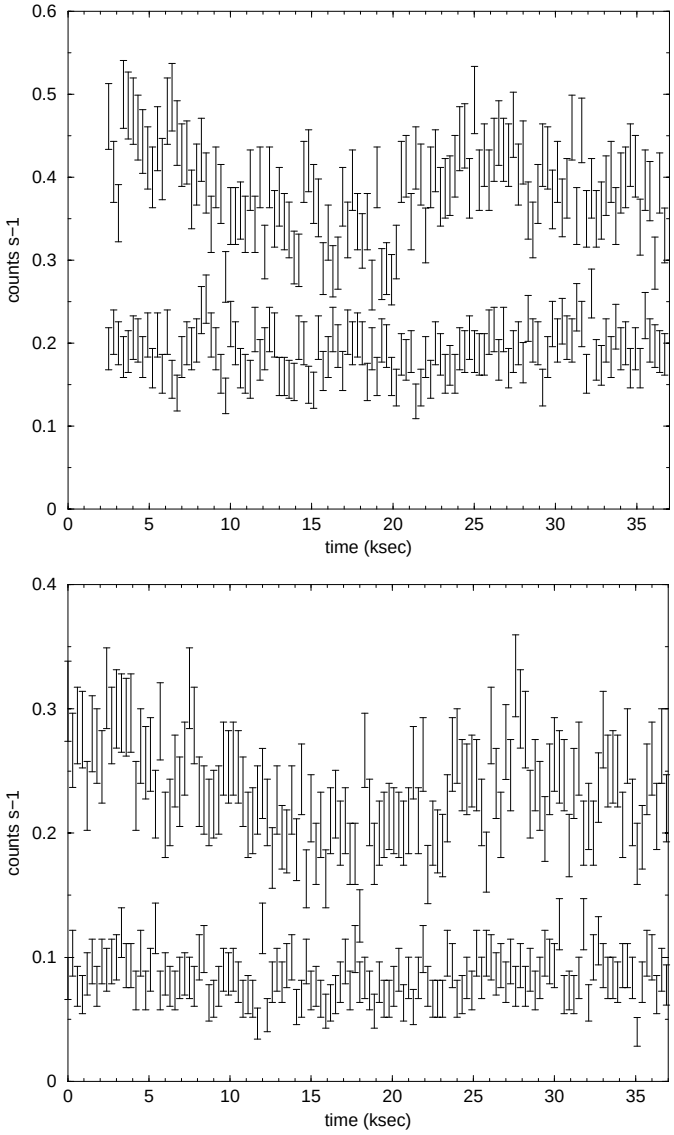

Fig. 1. Light curves of NGC 3227 obtained with the EPIC p−n (top) and the EPIC MOS (bottom) cameras in the 2–10 keV (upper curve) and in the 0.3–2 keV (lower curve) energy bands. The events are binned into 300 s time intervals.

The NGC 3227 light curves (see Fig. 1) do not show significant flux variations in the 0.3–2 keV band over the 37 ksec observation period. In contrast, count rate variations with an amplitude >40% are detected on a time scale of about 15 ksec in the high 2–10 keV energy band. This behaviour is illustrated in Fig. 2 which shows that the ratio of count rates in the high (HE; 2–10 keV) and low (LE; 0.3–2 keV) energy bands increases with the source flux. A high variability of NGC 3227 on time scales of hours−days has been previously reported in the literature. In particular, *XMM–Newton* observations are reminiscent

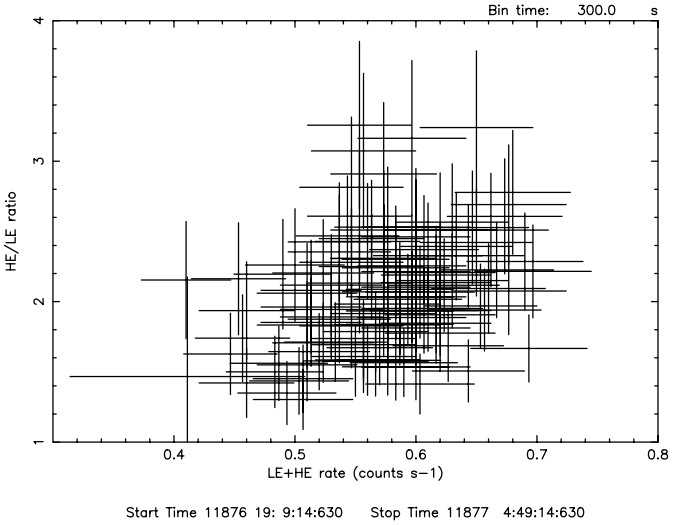

Fig. 2. Count rate ratio in the high (HE; 2–10 keV) and low (LE; 0.3–2 keV) energy bands as a function of the count rate in the entire EPIC 0.3–10 keV energy band. The events are binned into 300 s time intervals.

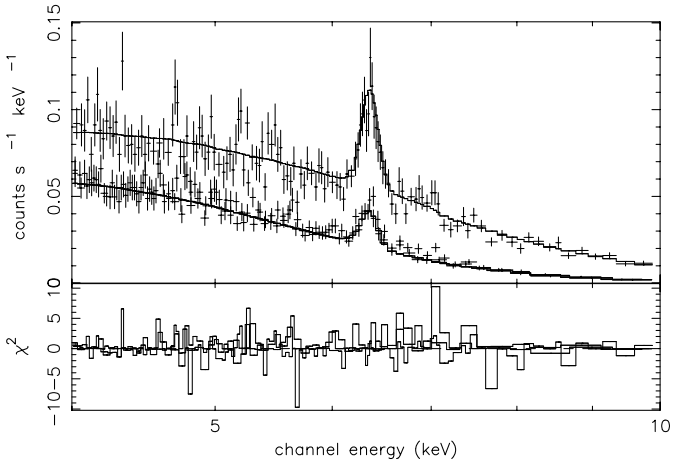

Fig. 3. Comparison of EPIC p−n and MOS data with a best fit model in the 4–10 keV energy range consisting of a powerlaw continuum and a Gaussian emission line.

of the 40% flux increase within 5 hours found in *HEAO1* data (Tennant & Mushotzky 1983) and of the differential variability between the *EXOSAT* LE (0.05–2 keV) and ME (2–10 keV) instruments (Turner & Pounds 1989).

4. Spectral analysis

4.1. Phenomenological model of the high energy continuum and Fe K spectral features

In order to parametrize the high energy spectrum of NGC 3227, we first consider a model in which a single power-law continuum is absorbed by the Galactic column density $N_{\rm H,0}^{\rm gal}$ and an additional screen of neutral material $N_{\rm H,z}^{\rm neu}$ at a redshift $z = 0.00386$. A statistically acceptable fit to the 4–10 keV spectral band excluding the 5–7 keV Iron K-shell region of NGC 3227 spectrum is obtained with a photon index $\Gamma = 1.55$. The best fit parameters are given in Table 1 (see Model A). If one extrapolates this power law to the 5–7 keV range, one sees an excess of emission around 6.4 keV in the observed reference frame. Therefore, we fitted the EPIC data in the 4–10 keV energy range by a phenomenological model consisting of an absorbed power law continuum and a Gaussian emission line (see Fig. 3). The best fit model to the EPIC p−n data points to the existence of an iron Kα fluorescence line at 6.39 ± 0.01 keV. The best fit Gaussian model to the line (see Table 1, Model B) indicates an equivalent width of $EW = 220 \pm 2$ eV. Since an emission line in Seyfert 1 galaxies is often associated with an absorption edge (e.g. Gondoin 2001a,b), we added an edge model to the redshifted Gaussian component. An absorption edge ($\tau = 0.07 \pm 0.06$) is detected at 7.6 ± 0.2 keV (see Table 1, Model C). The improvement in χ^2 fit statistics ($\Delta\chi^2/\Delta\nu = 2$ for 450 degree of freedom) is significant at >80% confidence using the F-statistic.

The most striking result of the spectral fit is the hardness of the continuum fit. The slope index that we obtained

Table 1. Phenomenological models of the NGC 3227 EPIC spectra in the 4−10 keV spectral band. Spectral fitting with model A does not include the 5–7 keV energy range.

Component	Parameters	Model A	Model B	Model C
WABS	$N_{\rm H,0}^{\rm gal}$ (cm^{-2})	2.1×10^{20}	2.1×10^{20}	2.1×10^{20}
ZWABS	$N_{\rm H,z}^{\rm neu}$ (cm^{-2})	$(7.1 \pm 2.2) \times 10^{20}$	$(7.1 \pm 1.3) \times 10^{20}$	$(7.3 \pm 1.6) \times 10^{20}$
ZPOWERLW	Γ	1.55 ± 0.14	1.52 ± 0.09	1.50 ± 0.13
	Norm	$(2.1 \pm 1.1) \times 10^{-3}$	$(2.0 \pm 0.6) \times 10^{-3}$	$(2.0 \pm 0.9) \times 10^{-3}$
ZGAUSS	E (keV)		6.39 ± 0.01	6.39 ± 0.01
	σ (eV)		53 ± 16	50 ± 17
	EW (eV)		220 ± 2	213 ± 2
ZEDGE	E (keV)			7.6 ± 0.2
	τ			0.07 ± 0.06
	χ^2_ν	0.97	1.04	1.04

($\Gamma \approx 1.5$) is comparable with the $\Gamma \approx 1.04-1.61$ values derived by George et al. (1998) from spectral fits of *ASCA* 1993 and 1995 data using different models (see Table 3 of their paper). Also, Reynolds (1997) found that the best fit power law model to the 2–10 keV spectral range of the *ASCA* spectrum of 1993 has a slope index $\Gamma = 1.30 \pm 0.01$ with no correction for absorption. An hypothesis not to be excluded is the existence of a broad underlying Fe Kα component which would amplify the absorption that we interpretate as an edge. If the red wing of this broad Kα component were present but not accounted for in the continuum fitting, it could tend to make the continuuum between 4 and 6 keV appear flatter. In order to test this hypothesis, we fitted the 3–10 keV spectrum of NGC 3227 with a power law, a narrow Gaussian emission component and a broad accretion disk line profile described by a DISKLINE (Fabian et al. 1989) or by a LAOR (Laor 1990) model. The DISKLINE model was used with a $(1 - (6/R)^{1/2})/R^3$ emissivity law. The LAOR model was tested with two values $\beta = 2$ and 3 for a power law dependence $R^{-\beta}$ of the emissivity. The disk inclination was fixed to 30° in both cases. The fits with the DISKLINE and LAOR models do not provide an acceptable description of the data ($\chi^2_\nu > 1.3$). Hence, we conclude that the

existence of an Fe K absorption edge at 7.6 keV is the most probable interpretation.

The iron Kα fluorescence line consists of two components Kα_1 and Kα_2 at 6.404 keV and 6.391 keV respectively for Fe I with a branching ratio of 2:1 (Bambynek et al. 1972). The natural width of the lines ($\Delta E \approx 3.5$ eV) and any broadening due to thermal motions of the emitting atoms ($\Delta E(\mathrm{eV}) \approx 0.4(T/10^6)^{1/2}$) are negligible compared to the energy resolution (155 eV *FWHM*) of the EPIC camera. The mean Fe Kα fluorescent line energy is an increasing function of ionization state. It rises slowly from 6.40 keV with Fe I to 6.45 keV in Fe XVII (neon-like) and then increases steeply with the escalating number of vacancies in the L-shell to 6.67 keV in Fe XXV and 6.9 keV in Fe XXVI (House 1969; Makishima 1986). The measured energy position of the NGC 3227 Fe K line at 6.39 ± 0.01 keV indicates that iron is in low states of ionization, say <Fe XVII.

The energy of the Fe absorption edge is also a function of the ionization stage of the Fe element. Aside from any blurring effect by the detector spectral response, the iron K edge is not expected to be sharp due to electron scattering and due to the presence of the iron Kβ line at 7.06 keV for Fe I. Hence, the exact measurement of its energy is difficult. In the case of Fe I, the K-shell absorption edge is at an energy $E_\mathrm{K} = 7.1$ keV, rising to 7.8 keV for Fe XVIII, and 9.3 keV for Fe XXVI (Morita & Fujita 1983). The measured energy of the NGC 3227 Fe K absorption edge at 7.6 ± 0.2 keV is consistent with the Fe Kα line position and indicates the presence of material where iron is in a range of low ionization states, up to Fe XVII.

4.2. Analysis of the soft energy range

Below 4 keV, a simultaneous fit of the EPIC MOS and p−n data with a power law spectrum indicates a strong absorption. A simple power law model with, cold, uniform, solar abundance absorption provides an unacceptable fit to the data. Hence, we fitted the EPIC MOS and pn spectra of NGC 3227 with a phenomenological model consisting of (i) a redshifted power law representing the primary continuum, (ii) Galactic absorption fixed at the level determined by the H I 21 cm measurements of 2.1×10^{20} cm^{-2} and (iii) a partial covering fraction absorption by neutral matter with cosmic abundance in the rest frame of the source. The photon index of the power law continuum was frozen to the value derived from the best fit power law models to the EPIC spectra above 4 keV (see Table 1). Absorption with a partial covering fraction of $92 \pm 1\%$ provides a barely acceptable fit to the data ($\chi^2_\nu = 1.22$) using the absorption cross-sections from Balucinska–Church & McCammon (1992) with a He cross-section based on Yan et al. (1998). The best fit model indicates the presence of a large column density of cold material ($N_\mathrm{H} = 6.5 \pm 0.1 \times 10^{22}$ cm^{-2}) in the line of sight to the nucleus. However, residuals to this model suggest an absorption contribution from ionized matter.

In order to quantify the column density of the ionized plasma, N_W, and the ionization parameter, ξ, of the ionized absorber, we fitted the EPIC spectra in the 0.3−10 keV range with a powerlaw model absorbed by neutral and ionized material. We first used the ionized absorber model ABSORI. In this single zone equilibrium ionization model the opacity of the gas is based on the ionization distribution of the relevant atomic species in a slab of Thomson-thin plasma as a function of the ionization parameter. This parameter is defined as $\xi = L/nR^2$, where n is the number density of the warm plasma and R the distance from the ionizing source with isotropic luminosity L in the interval 5 eV to 20 keV. The photon index of the incident power law continuum was frozen to the value derived from the best fit power law model to the EPIC spectra above 4 keV (see Table 1). The results of the spectral fitting (see Fig. 4) using a power law absorbed by neutral and ionized matter are given in Table 2. The best fit parameters ($\chi^2_\nu \approx 1.11$) to the EPIC spectra of NGC 3227 using a single zone warm absorber model give an ionization parameter $\xi = 50$ erg s^{-1} cm and a hydrogen column density $N_\mathrm{W} = (8.9 \pm 0.9) \times 10^{21}$ cm^{-2} for the ionized plasma. According to Kallman & Bautista (2001), the temperature of an optically photoionized gas in thermal equilibrium with a ionisation parameter $\xi = 50$ erg s^{-1} cm is around 10^5 K with only a small dependence on density over a wide range included between 10^6 cm^{-3} to 10^{16} cm^{-3}. Such a temperature leads to an acceptable description of the spectrum of NGC 3227.

The ABSORI model does not include X-ray emission by the ionized absorbing gas. Hence, we also used the XSTAR code (Kallman 2000) to model the transmitted and outward emitted spectrum of a spherical cloud illuminated by a central power law source. The XSTAR model assumes that all physical processes that affect the state of the gas are in steady state, i.e. the timescale for variation in the gas density and illuminating radiation are long compared with the timescales affecting all atomic processes and the propagation of radiation within the gas. The photoionization spectra depend a priori on (i) the shape of the photoionization continuum (ii) the elemental abundance, (iv) the particle density in the cloud, (v) the column density of the cloud and (vi) the ionization parameter. Test calculations show that the EUV spectral shape has no strong influence on the X-ray properties of the warm gas. Its ionization stage is dominated by the X-ray part of the incident continuum. We simulated the transmission and emission spectrum of a shell photoionized by a central power law source with an $E^{-1.52}$ energy dependence and a density fixed to $10^{9.5}$ cm^{-3}. The abundances were assumed to be solar. Spectra were generated for column densities ranging from 10^{19} cm^{-2} to 10^{22} cm^{-2} and ionization parameters ranging from 10 to 300 erg s^{-1} cm^{-2}. The best fit XSTAR model (see Table 2) gives an ionization parameter $\xi = 86$ erg s^{-1} cm and a hydrogen column density $N_\mathrm{W} = (2.7 \pm 0.7) \times 10^{21}$ cm^{-2} of the ionized plasma, comparable with those derived from the ABSORI model.

The *XMM–Newton* light curves (see Fig. 1) indicate significant flux variability in NGC 3227 above 2 keV on time scales of a few ksec. In order to identify the variable spectral components, we fitted the EPIC spectra during low and high count rate periods with a power law absorbed by neutral and ionized material. The low and high count rate periods are time intervals of 13 ksec extracted respectively in the middle and at the end of the observation period. The column densities of galactic neutral material and the energy of the Fe K line were fixed. The index and normalisation factor of the power law, the ionization

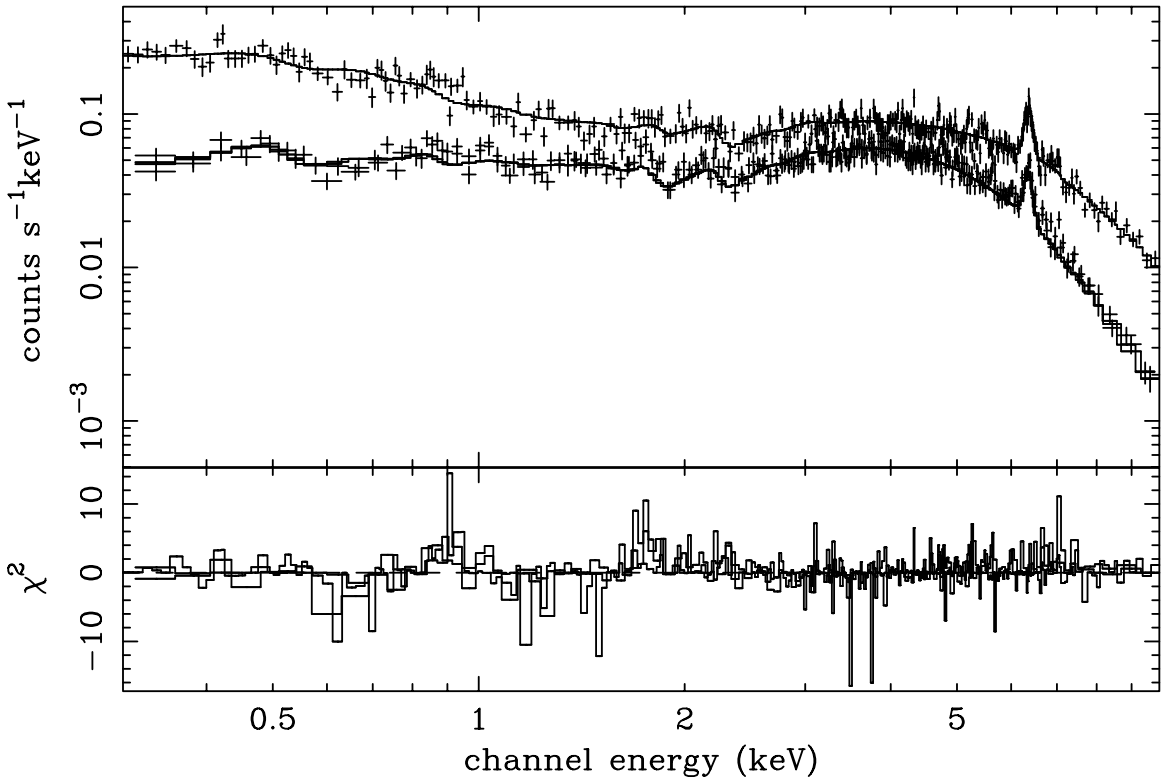

Fig. 4. Simultaneous fit of the EPIC pn, EPIC MOS 1 and EPIC MOS 2 spectra by a power law model absorbed by neutral and ionized gas (see Table 2). The model includes a Gaussian emission lines at 6.39 keV. The data and spectral fit are shown in the upper panel. The χ^2 distribution is displayed in the lower panel.

Table 2. Best fit parameters to the spectrum of NGC 3227 using either an ionized absorber model developed by Magdziarz & Zdziarski (1995) or photoionization spectra calculated with the XSTAR code (Kallman 2000).

Component	Parameters	ABSORI	XSTAR
WABS	N_H (cm^{-2}) (frozen)	2.1×10^{20} (frozen)	2.1×10^{20} (frozen)
ZPCFABS	$N_{H,z}^{neu}$ (cm^{-2})	$(6.6 \pm 0.1)\ 10^{22}$	$(6.3 \pm 0.1) \times 10^{22}$
	Covering frac.	$90 \pm 1\%$	$91 \pm 1\%$
ABS. MODEL	N_W (cm^{-2})	$8.9 \pm 0.9 \times 10^{21}$	$2.7 \pm 0.7 \times 10^{21}$
	Temperature (K)	1.2×10^5 (frozen)	
	ξ (erg s^{-1} cm)	50 ± 6	86 ± 5
ZPOWERLW	Γ	1.52	1.52
	χ^2	1172/1056 d.o.f. = 1.11	1267/1054 = 1.20

parameter and column density of the ionized absorber and the column density and covering fraction of the neutral absorber were left as free parameters. An excellent fit to both data sets is obtained. Changes in the neutral and ionized absorber parameters are not significant. The results suggest that short term variability in NGC 3227 might be due essentially to variations of the continuum emission. However, uncertainties in the determination of the power law slope and normalisation factor impede any conclusive statement.

The reflection grating spectrometers RGS on board *XMM–Newton* are well suited to identify absorption and emission lines at low energy since they have a higher spectral resolution than the EPIC cameras. Unfortunately, the low signal to noise ratio of the RGS spectra of NGC 3227 does not enable us to perform any diagnosis.

5. Discussion

The EPIC MOS and p−n spectra show an emission line at 6.4 keV and an absorption edge around 7.6 keV. Spectral fitting of EPIC data with the PEXRAV model of a power law spectrum reflected from neutral material (Magdziarz & Zdziarski 1995) shows no significant evidence for a reflection component in NGC 3227. However, Ginga observations (Nandra & Pounds 1994) provided circumstantial evidence for a reflection fraction greater than 0.5 (George & Fabian 1991). Within the frame of such a model, the Fe Kα emission and the absorption edge in the EPIC spectrum could be produced by Compton reflection of a primary continuum onto an accretion disk. Possible contributions to these reflection components may come from material within the accretion disk itself (Pounds et al. 1990) or

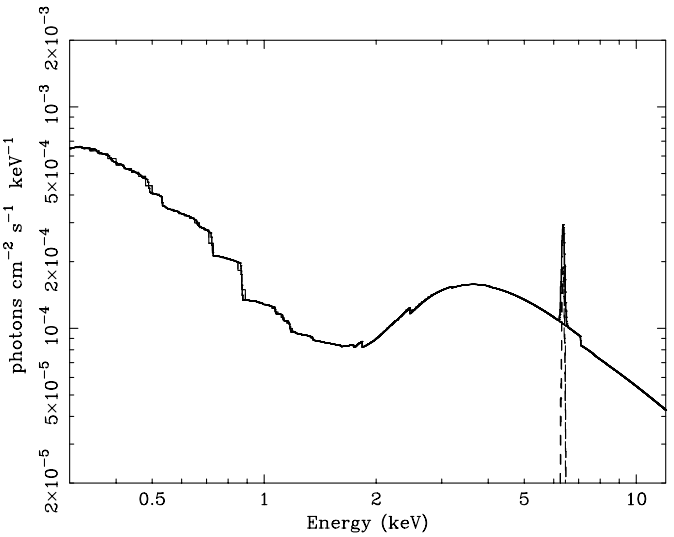

Fig. 5. Spectral model of NGC 3227. The model is the same as the one displayed in the count rate spectrum of Fig. 4.

from matter further out (Krolik et al. 1994; Ghisellini et al. 1994). Fe K lines in many AGNs are observed to be several tens of thousands of km s^{-1} broad and significantly redshifted (Mushotzky et al. 1995; Tanaka et al. 1995; Page et al. 2001; Gondoin et al. 2002). Orbital motion deep in a relativistic gravitational potential seems to be the only interpretation for line profiles of that sort. Other AGNs show narrow Fe K lines (Reeves et al. 2001a; Yaqoob et al. 2001; Gondoin et al. 2001a,b). Also, a unique iron K emission line profile with two distinct components has been recently reported (Reeves et al. 2001b) in Mrk 205. The Fe K emission line that we detected in NGC 3227 is narrow suggesting contribution from material in low ionization states relatively far from a central black hole. The energy position of the Fe K line at 6.39 ± 0.01 keV indicates that iron is in low states of ionization. The gas of the reflection slab would apparently remain essentially cool despite being exposed to an intense flux of X-rays. Such a result can be interpreted as an indication that the gas in the putative accretion disk is dense (Guilbert & Rees 1988; Ferland & Rees 1988).

An alternative explanation to the Fe K complex invokes partial covering of the X-ray source by cold, dense material. To produce a line width of about 200 eV, as observed in the present object, this cold medium should have a column density of iron greater than 10^{23} H atoms cm^{-2} (for solar abundances) in the case of a homogeneous and spherical distribution (Inoue 1985). Our *XMM–Newton* observation of NGC 3227 performed in November 2000 shows that the spectrum above 4 keV can be adequately described by a power law continuum with $\Gamma \approx 1.5$. The spectrum at lower energies is heavily absorbed by neutral gas with a hydrogen column density $N_{\rm H} \approx 6{-}7 \times 10^{22}$ cm^{-2} and a covering fraction of about 90%. A smaller fraction of the flat continuum is attenuated due to the presence of ionized material ($N_{\rm W} \approx 2{-}9 \times 10^{21}$ cm^{-2}) intrinsic to NGC 3227. X-ray spectra of AGNs commonly reveal intrinsic absorption by highly ionized or "warm" gas. The location of this gas is still unknown. Suggestions range all the way from the broad line region (BLR) possibly as close as 0.01 pc from the nucleus, to distances of 10 pc or more. Rapid apparent column density variations have been interpreted as suggesting locations within the BLR (Reynolds et al. 1995). On the other hand the same data also indicate that at least some of the gas may be much further away (Otani et al. 1996). Morales et al. (2000) suggested that the absorber is spread all the way from less than 0.05 pc to more than 1 pc. Still less is known about the origin of the gas producing warm absorber features. Some of the diverse suggestions include evaporation off "bloated stars" in the BLR (Netzer 1996) gas, evaporation off the torus obscuring the nucleus, that becomes the scattering gas seen in type 2 Seyfert galaxies (Krolik & Kriss 1995), and a wind driven off the accretion disk (Elvis 2000; Bottorff et al. 2000). These conclusion are often based on the most commonly observed features associated with O VII and O VIII (Reynolds 1997; George et al. 1998). In order to make them reasonably abundant, many photoionization models of warm absorbers suggest that ξ is in the range 10–100 erg s^{-1} cm (e.g. Brandt et al. 1997; Reynolds 1997; George et al. 1998; Mathur et al. 1997). Our analysis of *XMM–Newton* data also indicates the presence of a substantial amount of gas with $\xi \approx 50{-}90$ erg s^{-1} cm in the nucleus of NGC 3227. Using a primary continuum with a power law index $\Gamma = 1.52$ (see Table 1, Model B), we calculated a ionizing luminosity $L_{\rm ion} = 6.3 \times 10^{41}$ erg s^{-1} in the 1–1000 Rydberg range for a distance of 15.4 Mpc ($z = 0.00386$ and $H_0 = 75$ km s^{-1} Mpc^{-1}). Under the assumption that the species involved are in ionization balance, this leads to an estimate of the maximum distance of the ionized absorbing region $r_{\rm max} \approx 30 \times L_{\rm ion,44} \times N_{22}^{-1} \times \xi_{100}^{-1}$ pc (Krolik & Kriss 2001), i.e. $r_{\rm max} \approx 0.45$ pc for $L_{\rm ion,44} \approx 6 \times 10^{-3}$, $N_{22}^{-1} \approx 0.6$ and $\xi_{100} \approx 0.7$ where the fiducial quantities (10^{44} ergs s^{-1} for $L_{\rm ion}$, 10^{22} cm^{-2} for N and 100 for ξ) are representative of those commonly inferred for AGNs.

The continuum X-ray emission of NGC 3227 as observed by *XMM–Newton* is spectrally harder than seen in the majority of Seyfert 1 galaxies ($\Gamma \approx 1.9$; Nandra & Pounds 1994), consistent with the findings of most previous measurements of the source (Turner & Pounds 1989; Turner et al. 1991; Weaver et al. 1995; George et al. 1998). During the *XMM–Newton* observations, the luminosity was lower than during previous measurements by *HEAO–1* (Weaver et al. 1995), *Einstein* (Turner et al. 1991), *EXOSAT* (Turner & Pounds 1989), *Ginga* (Nandra & Pound 1994) and *ASCA* (Ptak et al. 1994; George et al. 1998). Comparisons with *ASCA* observations performed in 1993 and 1995 indicate a similar or lower column density of ionized absorber but a higher column density of absorbing neutral material during *XMM–Newton* observations. This suggests that the transit of clouds of neutral or weakly ionized material across the line of sight to the source could explain the low X-ray luminosity of NGC 3227 during *XMM–Newton* observation. Some previous observations of NGC 3227 (e.g. Reichert et al. 1985) also favored a partial covering model. Recent *Chandra* LETGS observations carried out in October 2000 can also be accounted for by the presence of a warm absorber and a partial coverer with a column density of $N_{\rm H} \approx 2.5{\times}10^{22}$ cm^{-2} (Komossa 2001). This value is comparable with the column density of neutral material ($N_{\rm H} \approx 6{-}7 \times 10^{22}$ cm^{-2}) that we derived from the *XMM–Newton* observation performed one month later. These column densities are two orders of

magnitude higher than the value measured by Komossa et al. (1997) using *ROSAT* PSPC observations performed in May 1993. Assuming Galactic dust properties and dust/gas ratio, these values obtained recently are higher than the column density required to account for the reddening $E_{B-V} = 0.51 \pm 0.04$ derived by Cohen (1983) from the narrow Hα/Hβ ratio (cf. Shull & van Steenberg 1985). They could also explain the somewhat larger $E_{B-V} = 0.94 \pm 0.23$ but less reliable reddening derived from the [S II] lines (Cohen 1983). However, the small amount of cold absorption measured from an *HST* UV spectrum of NGC 3227 (Crenshaw et al. 2001) taken approximately 9 months prior to the *XMM–Newton* and *Chandra* observations suggests that cold absorption is variable on a timescale of months in NGC 3227. It is worth noting that variable absorption columns of cold material are common among Seyfert 2 galaxies (Risaliti et al. 2001). For a subsample of sources observed at least five times, these authors find that the typical variation time is less than a year for moderately and heavily absorbed ($N_{\rm H} > 10^{22}$ cm^{-2}) sources. This seems also to hold for the intermediate type Seyfert galaxy NGC 3227 where rapid variability on a timescale of a few ksec could be related to variations of the continuum emission while variability on a timescale of weeks and months also involves changes in the column density of neutral absorbing material. Assuming that the typical timescale of variation corresponds to the crossing time of a discrete cloud along the line of sight, significant variability of the cold absorption ($\Delta N_{\rm H} \approx 4 \times 10^{22}$ cm^{-2}) on a time scale of a month between the *Chandra* and *XMM–Newton* observations suggests the presence of clumpy circumnuclear neutral material on a scale well below a parsec (Risalti et al. 2002), within the maximum distance of the ionized absorbing region. Within the standard AGN model, X-ray absorption by cold gas would be located much nearer to the central black hole than the standard torus. Using spectral and dynamical constraints, Uttley et al. (2002) argue that they witnessed in early 2001 broad line region clouds passing the line of sight to the nucleus. Testing correlations between reddening indicators and X-ray absorbing column densities on timescale of weeks/months is needed to further constrain the location and kinematics of absorbing clouds along the line of sight to NGC 3227.

Acknowledgements. We thank our colleagues from the *XMM–Newton* Science Operation Centers for their support in implementing the observations. We are grateful to the anonymous referee for the improvements brought to an earlier version of the manuscript.

References

Bambynek, W., Craseman, B., Fink, R. W., et al. 1972, Rev. Mod. Phys., 44, 716
Balucinska–Church, M., & McCammon, D. 1992, ApJ, 400, 699
Bottorff, M. C., Korista, K. T., & Shlosman, I. 2000, ApJ, 537, 134
Brandt, W. N., Mathur, S., Reynolds, C. S., & Elvis, M. 1997, MNRAS, 292, 407
Cohen, R. D. 1983, ApJ, 273, 489
Courvoisier, T. J., & Paltani, S. 1992, IUE-Uniform Low Dispersion Archive Access Guide No. 4, ESA-SP 1153A/B (Noordwijk: ESA)
Crenshaw, D. M., Kraemer, S. B., Bruhweiler, F. C., & Ruiz, J. R. 2001, ApJ, 555, 633
Elvis, M. 2000, ApJ, 545, 63
Fabian, A. C., Rees, M. J., Stella, L., et al. 1989, MNRAS, 238, 729
Ferland, G. J., & Rees, M. J. 1988, ApJ, 332, 141
George, I. M., Nandra, K., & Fabian, A. C. 1990, MNRAS, 242, 28
George, I. M., & Fabian, A. C. 1991, MNRAS, 249, 352
George, I. M., Turner, T. J., & Netzer, H. 1995, ApJ, 438, L67
George, I. M., Mushotzky, R., Turner, T. J., et al. 1998, ApJ, 509, 146
Ghisellini, G., Haardt, F., & Matt, G. 1994, MNRAS, 267, 743
Gondoin, P., Aschenbach, B., Erd, C., et al. 2000, SPIE Proc., 4140, 1
Gondoin, P., Lumb, D., Siddiqui, H., et al. 2001a, A&A, 373, 805
Gondoin, P., Barr, P., Lumb, D., et al. 2001b, A&A, 378, 806
Gondoin, P., Orr, A., Lumb, D., & Santos-Lleo, M. 2002, A&A, 388, 74
Guilbert, P. W., & Rees, M. J. 1988, MNRAS, 233, 475
den Herder, J. W., Brinkman, A. C., Kahn, S. M., et al. 2001, A&A, 365, L7
House, L. L. 1969, ApJS, 18, 21
Inoue, H. 1985, in Japan−US Seminar on Galactic and Extragalactic Compact X-Ray Sources, ed. Y. Tanaka, & W. H. G. Lewin (Tokyo: ISAS), 283
Jansen, F., Lumb, D., Altieri, B., et al. 2001, A&A, 365, L1
Kallman, T. R. 2000, XSTAR User's guide, version 2.1 (Greenbelt, M.D.: NASA: GSFC)
Kallman, T., & Bautista, M. 2001, ApJS, 133, 221
Komossa, S., & Fink, H. 1997, A&A, 327, 483
Komossa, S., Burwitz, V., Predehl, P., & Kaastra, J. 2001, in The Central Kiloparsec of Starbursts and AGNs, ed. J. H. Knapen, J. E. Beckman, I. Shlosman, & T. J. Mahoney, ASP Conf. Ser., 249, 411
Kraemer, S. B., George, I. M., Turner, T. J., & Crenshaw, D. M. 2000, ApJ, 535, 53
Krolik, J. H., Madau, P., & Zycki, P. 1994, ApJ, 420, L57
Krolik, J. H., & Kriss, G. A. 1995, ApJ, 447, 512
Krolik, J. H., & Kriss, G. A. 2001, ApJ, 561, 684
Laor, A. 1991, ApJ, 376, 90
Magdziarz, P., & Zdziarski, A. 1995, MNRAS, 273, 837
Makishima, K. 1986, in The Physics of Accretion onto Compact Objects, ed. K. O. Mason, M. G. Watson, & N. E. White (Springer Verlag, Berlin), 250
Mathur, S., Wilkes, B., & Aldcroft, T. 1997, ApJ, 478, 182
Mattews, W. G., & Ferland, G. J. 1987, ApJ, 323, 456
Morita, S., & Fujita, J. 1983, J. Phys. Soc. Japan, 52, 1957
Morales, R., Fabian, A. C., & Reynolds, C. S. 2000, MNRAS, 315, 149
Mundell, C. G., Pedlar, A., Axon, D. J., et al. 1997, MNRAS, 277, 641
Murphy, E. M., Lockman, F. J., Laor, A., & Elvis, M. 1996, ApJS, 105, 369
Mushotzky, R. F., Fabian, A. C., Iwasawa, K., et al. 1995, MNRAS, 272, L9
Nandra, K., & Pounds, K. A. 1994, MNRAS, 268, 405
Netzer, H., Turner, T. J., & George, I. M. 1994, ApJ, 435, 106
Netzer, H. 1996, ApJ, 473, 781
Oosterbrock, D. E., & Martel, A. 1993, ApJ, 414, 552
Otani, C., Kii, T., Reynolds, C. S., et al. 1996, PASJ, 48, 211
Page, M. J., Mason, K. O., Carrera, F. J., et al. 2001, A&A, 365, L152
Pounds, K. A., Nandra, K., Stewart, G. C., & Leighly, K. 1989, MNRAS, 240, 769
Pounds, K. A., Nandra, K., Stewart, G. C., et al. 1990, Nature, 344, 132
Ptak, A., Yaqoob, T., Serlemitsos, P. J., & Mushotsky, R. 1994, ApJ, 436, L31

Reeves, J. N., Turner, M. J. L., Bennie, P. J., et al. 2001a, A&A, 365, L116
Reeves, J. N., Turner, M. J. L., Pounds, K. A., et al. 2001b, A&A, 365, L134
Reichert, G. A., Mushotzky, R. F., Petre, R., et al. 1985, ApJ, 296, 69
Reynolds, C. S., Fabian, A. C., Nandra, K., et al. 1995, MNRAS, 277, 901
Reynolds, C. S. 1997, MNRAS, 286, 513
Risaliti, G., Elvis, M., & Nicastro, F. 2002, ApJ, 571, 234
Rush, B., Malkan, M., Fink, H. H., & Voges, W. 1996, ApJ, 471, 490
Shull, J. M., & van Steenberg, M. E. 1985, ApJ, 294, 599
Strüder, L., Briel, U., Dennerl, K., et al. 2001, A&A, 365, L18
Tanaka, Y., Nandra, K., & Fabian, A. C. 1995, Nature, 375, 659
Tennant, A. F., & Mushotzky, R. F. 1983, ApJ, 264, 92
Turner, T. J., & Pounds, K. A. 1989, MNRAS, 240, 830
Turner, T. J., Weaver, K. A., Mushotzsky, R. F., et al. 1991, ApJ, 381, 85
Turner, M. J. L. T., Abbey, A., Arnaud, M., et al. 2001, A&A, 365, L27
Uttley, P., Lamer, G., & McHardy, I. M. 2002, in Active Galactic Nuclei: from Central Engine to Host Galaxy, ed. S. Collin, F. Combes, & I. Shlosman, ASP Conf. Ser., 33
Weaver, K. A., Arnaud, K. A., & Mushotzsky, R. F. 1995, ApJ, 447, 121
Winge, C., Peterson, B. M., Horne, K., et al. 1995, ApJ, 445, 680
Yan, M., Sadeghpour, H. R., & Dalgarno, A. 1998, ApJ 496, 1044
Yaqoob, T., George, I. M., Nandra, K., et al. 2001, ApJ, 546, 759